Acta Crystallographica Section B
Structural Science
ISSN 0108-7681

Structural studies on C-amidated amino acids and peptides: structures of hydrochloride salts of C-amidated Ile, Val, Thr, Ser, Met, Trp, Gln and Arg, and comparison with their C-unamidated counterparts

Yasuko In,* Mayumi Fujii, Yasuhiro Sasada and Toshimasa Ishida

Osaka University of Pharmaceutical Sciences, 4-20-1 Nasahara, Takatsuki, Osaka 569-1094, Japan

Correspondence e-mail: in@oysun01.oups.ac.jp

Received 27 May 2000
Accepted 9 October 2000

To elucidate the structural features of amino acids caused by the C-terminal α-amidation, the crystal structures of HCl salts of C-terminal amidated Ile, Val, Thr, Ser, Met, Trp, Gln and Arg were analysed and compared with those of their C-terminal free acids. The bonding parameter of the amide group was little affected by the different chemical properties of the side chains. As for the molecular packing patterns, some structural differences were observed by the C-amidation. The Cα—H$\cdots$O hydrogen bonds and carbonyl–carbonyl interactions were more strengthened by the salt formation with HCl in C-amides than C-acids. Furthermore, there is a clear difference between the interaction patterns with Cl ions. In most C-amide crystals, Cl ions are bifurcately hydrogen-bonded to two neighbouring amide NH_2 groups and the parallel layers of the C-amides and Cl ions are alternatively formed. In the case of the carboxyl OH in C-acid crystals, however, the direct hydrogen bond with the Cl ion is not always observed and is largely dependent on the crystal packing environment. This suggests the superior hydrogen-bonding ability of NH$\cdots$Cl$^-$ compared with OH$\cdots$Cl$^-$. The difference in hydrogen-bonding ability between the amide and carboxyl groups is considered, based on the spatial dispositions of the hydrogen-bonding polar atoms/groups.

1. Introduction

The majority of mammalian and insect peptide hormones possess a C-terminal α-amide (hereafter named C-amide), as exemplified by calcitonin, cholecystokinin, gastrin, neurokinins, neuropeptides, substance P and their related peptides (Eipper & Mains, 1988). The C-amide is essential to express the bioactivity and the glycine-extended or C-terminal free acid (hereafter named C-acid) analogues of the α-amidated peptides lead to considerable loss of activity (Merkler, 1994; Suwan *et al.*, 1994).

At present, the biological/structural function of the C-amide is far from the full understanding, although the amidation arises from the oxidative cleavage of C-terminal glycine-extended prohormones (Kulathila *et al.*, 1999). The molecular conformation of the bioactive peptide and/or the interaction with the receptor would be affected by the difference between C-acid and -amide groups. Thus, it appears important to examine the difference between the stable conformations of C-amide and -acid peptides, and between their interaction modes with neighbouring molecules; the information would be useful on considering the binding specificity of the C-amide peptide to the receptor.

As part of the series elucidating structural features by C-terminal amidation (In *et al.*, 2000), we have analysed the crystal structures of HCl salts of the following C-amides, *i.e.* $IleNH_2$, $ValNH_2$, $ThrNH_2$, $SerNH_2$, $MetNH_2$, $TrpNH_2$, $GlnNH_2$ and $ArgNH_2$ (Fig. 1). In this paper we report their molecular and crystal structures, and discuss the difference between their intermolecular interactions and those of the corresponding C-acids. Since the Cl anion exists in the living cell, such information may be useful on understanding the different biological function between the C-amide and -acid peptides.

2. Experimental

The respective C-amides were purchased from Peptide Institute Inc. (Osaka, Japan). The crystallization solvents, crystal densities (measured by the flotation method using a CCl_4–C_6H_6 mixture), crystallographic data and structure refinements are summarized in Table 1.

All X-ray crystallographic data were obtained using a Rigaku AFC-5 diffractometer with graphite-monochromated Cu $K\alpha$ radiation (λ = 1.5418 Å) and a 12 kW rotating anode generator. Cell refinement, data collection and data reduction were performed using the *MSC/AFC* software (Molecular Structure Corporation, 1991). Unit-cell dimensions were determined by a least-squares fit of 2θ angles of 25 reflections in the range $45 < 2\theta < 55°$. Intensity data were collected at 293 K in an ω–2θ scan mode; the backgrounds were counted for 5 s at both extremes of each reflection peak. The weak intensities were rescanned (up to seven scans) to ensure good counting statistics. The absorption corrections by the ψ-scan method (North *et al.*, 1968) were applied, except $ValNH_2$·HCl. The observed intensities were corrected for the Lorentz and polarization effects. Four standard reflections were monitored every 100 reflections throughout the data collection, showing a random variation of $< \pm 2\%$ without significant trends.

The obtained bond lengths and angles were all within acceptable region, and no abnormality/uncertainty was observed.[1] All numerical calculations were carried out at the Computer Centre, Osaka University of Pharmaceutical Sciences.

In order to compare the observed bonding parameters and crystal packings of the present C-amides with those of the corresponding C-acids, the following CSD (Cambridge Structural Database) data were used: IleOH·HCl (LILEUC10; Varughese & Srinivasan, 1976), Ile (LISLEU02; Görbitz & Dalhus, 1996), ValOH·HCl (VALEHC10; Ando *et al.*, 1967; VALEHCl1; Koetzle *et al.*, 1974), Val (LVALIN01; Dalhus & Gorbitz, 1996), Thr (LTHREO01; Ramanadham *et al.*, 1973), Ser (LSERIN01; Kistenmacher *et al.*, 1974), MetOH·HCl (METHCL; Blasio *et al.*, 1977), Met (LMETON10; Torii & Iitaka, 1973), TrpOH·HCl (TRYPTC; Takigawa *et al.*, 1966), GlnOH·HCl (GLUTAN; Shamala & Venkatesan, 1972), Gln (GLUTAM01; Koetzle *et al.*, 1973), and $ArgO^-$·HCl (ARGHCL10; Dow *et al.*, 1970), where the neutral and anionic states of C-terminal carboxyl group are represented by OH and O^-, respectively, and the zwitterionic states of amino acid are represented by the usual three-letter symbols.

3. Results and discussion

3.1. Molecular structure and conformation

Some selected bond lengths and angles, and torsion angles defining the molecular conformations of C-amides are summarized in Tables 2 and 3, respectively, where the corresponding data of C-acids are also given for comparison. All the C-amides take the protonated NH_3^+ form by salt formation with HCl, thus the molecule is in a monocationic state; $ArgNH_2$ has the dicationic form protonated at the amino and guanidium groups, and is neutralized by two HCl molecules. Since the HCl salts of C-acids take a similar monocationic state as the protonated NH_3^+ and the neutral COOH, the comparison between their bonding parameters would reflect the structural feature of the amide and carboxyl groups.

As judged from the standard deviations of the averaged bond lengths and angles listed in Table 2, it could be suggested that the amide group takes the rigid structure and is not significantly influenced by chemical differences in the side chain. This is in contrast with the carboxyl group, which allows a relatively large deformation for the bond angle, together with the rather short C1′═O1′ bond length.

The conformational torsion angles of C-amides are all in either of the regions acceptable for the usual amino acids (Cody, 1985), although some of them deviate somewhat from the most preferred angle. The torsion angle of ψ is determined by the relative disposition between the cationic NH_3^+ and electronegative carbonyl O1′ atoms, and appears to be highly affected by the intermolecular interaction with the neighbouring molecules. When these torsion angles are compared with those of C-acids and their HCl salts (Table 3), no notable conformational feature caused by the C-amidation could be

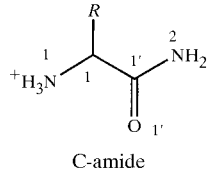

	R
Ile	-CH(CH$_3$)(C$_2$H$_5$)
Val	-CH(CH$_3$)$_2$
Thr	-CH(OH)(CH$_3$)
Ser	-CH$_2$OH
Met	-CH$_2$CH$_2$SCH$_3$
Trp	-CH$_2$ 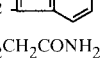
Gln	-CH$_2$CH$_2$CONH$_2$
Arg	-CH$_2$CH$_2$CH$_2$NHC(NH$_2$)$_2$

Figure 1
Chemical structures and atomic numberings of C-amides and C-acids, together with those of the side chains of Ile, Val, Thr, Ser, Met, Trp, Gln and Arg.

[1] Supplementary data for this paper are available from the IUCr electronic archives (Reference: OA0030). Services for accessing these data are described at the back of the journal.

Table 1
Experimental details.

	$IleNH_2$·HCl	$ValNH_2$·HCl	$ThrNH_2$·HCl	$SerNH_2$·HCl
Crystal data				
Chemical formula	$C_6H_{15}N_2O^+\cdot Cl^-$	$C_5H_{13}N_2O^+\cdot Cl^-$	$C_4H_{11}N_2O_2^+\cdot Cl^-$	$C_3H_9N_2O_2^+\cdot Cl^-$
Chemical formula weight	166.65	152.62	154.6	140.57
Cell setting, space group	Monoclinic, $P2_1$	Monoclinic, $P2_1$	Orthorhombic, $P2_12_12_1$	Monoclinic, $P2_1$
a, *b*, *c* (Å)	7.5775 (13), 4.8971 (13), 12.5686 (14)	5.3377 (8), 7.4572 (9), 9.899 (1)	10.1624 (15), 10.5673 (17), 6.749 (3)	7.562 (2), 4.9986 (18), 8.519 (3)
β (°)	94.195 (12)	91.73 (1)	90	90.76 (3)
V (Å^3)	465.14 (16)	393.84 (9)	724.8 (3)	322.00 (18)
Z	2	2	4	2
D_x (Mg m^{-3})	1.190	1.287	1.417	1.450
D_m (Mg m^{-3})	1.221 (5)	1.280 (5)	1.402 (5)	–
Density measured by	Measured	Measured	Measured	–
Radiation type	Cu $K\alpha$	Cu $K\alpha$	Cu $K\alpha$	Cu $K\alpha$
No. of reflections for cell parameters	25	25	25	25
θ range (°)	0.3–65.02	0.3–65.01	0.3–63.10	0.3–67.40
μ (mm^{-1})	3.199	3.731	4.173	4.639
Temperature (K)	293 (2)	293 (2)	293 (2)	293 (2)
Crystal form, colour	Plate, colourless	Plate, colourless	Cubic, colourless	Plate, colourless
Crystal size (mm)	0.6 × 0.4 × 0.05	0.8 × 0.6 × 0.3	0.8 × 0.6 × 0.6	0.8 × 0.2 × 0.05
Data collection				
Diffractometer	Rigaku AFC-5*R*	Rigaku AFC-5*R*	Rigaku AFC-5*R*	Rigaku AFC-5*R*
Data collection method	ω–2θ scans	ω–2θ scans	ω–2θ scans	ω–2θ scans
Absorption correction	ψ-scan	None	ψ-scan	ψ-scan
T_{min}	0.629	–	0.782	0.464
T_{max}	0.999	–	0.999	0.793
No. of measured, independent and observed reflections	963, 893, 817	1458, 731, 718	710, 710, 710	687, 638, 626
Criterion for observed reflections	$I > 2\sigma(I)$	$I > 2\sigma(I)$	$I > 2\sigma(I)$	$I > 2\sigma(I)$
R_{int}	0.0518	0.1353	0.0000	0.0499
θ_{max} (°)	65.02	65.01	63.10	67.40
Range of *h*, *k*, *l*	$0 \rightarrow h \rightarrow 8$ $-5 \rightarrow k \rightarrow 0$ $-14 \rightarrow l \rightarrow 14$	$-6 \rightarrow h \rightarrow 6$ $-8 \rightarrow k \rightarrow 0$ $-11 \rightarrow l \rightarrow 11$	$0 \rightarrow h \rightarrow 11$ $0 \rightarrow k \rightarrow 12$ $-7 \rightarrow l \rightarrow 0$	$0 \rightarrow h \rightarrow 9$ $0 \rightarrow k \rightarrow 5$ $-10 \rightarrow l \rightarrow 10$
No. and frequency of standard reflections	3, every 100 reflections	3, every 100 reflections	3, every 100 reflections	3, every 100 reflections
Intensity decay (%)	2	2	2	2
Refinement				
Refinement on	F^2	F^2	F^2	F^2
$R[F^2>2\sigma(F^2)]$, $wR(F^2)$, S	0.0688, 0.1872, 1.659	0.0369, 0.0967, 0.747	0.0471, 0.1210, 1.098	0.0499, 0.1619, 1.582
No. of reflections and parameters used in refinement	893, 90	731, 82	710, 83	638, 73
H-atom treatment	Mixed	Mixed	Mixed	Mixed
Weighting scheme	$w = 1/[\sigma^2(F_o^2) + (0.1P)^2]$, where $P = (F_o^2 + 2F_c^2)/3$	$w = 1/[\sigma^2(F_o^2) + (0.1P)^2]$, where $P = (F_o^2 + 2F_c^2)/3$	$w = 1/[\sigma^2(F_o^2) + (0.0986P)^2 + 0.4071P]$, where $P = (F_o^2 + 2F_c^2)/3$	$w = 1/[\omega^2(F_o^2) + (0.1P)^2]$, where $P = (F_o^2 + 2F_c^2)/3$
$(\Delta/\sigma)_{max}$	0.094	0.176	0.049	0.003
$\Delta\rho_{max}$, $\Delta\rho_{min}$(e Å^{-3})	0.699, −0.289	0.298, −0.407	0.496, −0.589	0.421, −0.497
Extinction method	None	*SHELXL*	*SHELXL*	*SHELXL*
Extinction coefficient	–	0.67 (4)	0.34 (2)	0.050 (14)

	$MetNH_2$·HCl	$TrpNH_2$·HCl	$GlnNH_2$·HCl	$ArgNH_2$·HCl
Crystal data				
Chemical formula	$C_5H_{13}N_2OS^+\cdot Cl^-$	$C_{11}H_{14}ClN_3O$	$C_5H_{12}N_3O_2^+\cdot Cl^-$	$C_6H_{19}N_5O_2^{2+}\cdot 2Cl^-$
Chemical formula weight	184.68	239.7	181.63	264.16
Cell setting, space group	Monoclinic, $P2_1$	Monoclinic, $P2_1$	Monoclinic, $P2_1$	Orthorhombic, $P2_12_12_1$
a, *b*, *c* (Å)	7.591 (3), 5.029 (3), 11.786 (4)	7.6394 (11), 5.2786 (13), 14.5967 (14)	7.741 (2), 4.8907 (13), 10.8159 (10)	7.536 (3), 32.487 (3), 5.277 (4)
β (°)	96.49 (3)	100.047 (10)	94.180 (13)	90
V (Å^3)	447.0 (4)	579.59 (17)	408.39 (16)	1291.9 (10)
Z	2	2	2	4
D_x (Mg m^{-3})	1.372	1.374	1.477	1.358
D_m (Mg m^{-3})	–	1.362 (5)	1.462 (5)	1.366 (5)
Density measured by	–	Measured	Measured	Measured

Table 1 (continued)

	$MetNH_2$·HCl	$TrpNH_2$·HCl	$GlnNH_2$·HCl	$ArgNH_2$·HCl
Radiation type	Cu $K\alpha$	Cu $K\alpha$	Cu $K\alpha$	Cu $K\alpha$
No. of reflections for cell parameters	25	25	25	25
θ range (°)	0.3–67.48	0.3–65.03	0–67.61	0.3–67.61
μ (mm^{-1})	5.511	2.782	3.832	4.491
Temperature (K)	293 (2)	293 (2)	293 (2)	293 (2)
Crystal form, colour	Plate, colourless	Needle, colourless	Needle, colourless	Plate, colourless
Crystal size (mm)	0.7 × 0.2 × 0.05	0.5 × 0.2 × 0.2	0.8 × 0.2 × 0.2	0.5 × 0.25 × 0.1
Data collection				
Diffractometer	Rigaku AFC-5*R*	Rigaku AFC-5*R*	Rigaku AFC-5*R*	Rigaku AFC-5R
Data collection method	ω–2θ scans	ω–2θ scans	ω–2θ scans	ω–2θ scans
Absorption correction	ψ-scan (North *et al.*, 1968)	ψ-scan	ψ-scan	ψ-scan
T_{min}	0.697	0.329	0.355	0.288
T_{max}	0.759	0.573	0.465	0.998
No. of measured, independent and observed reflections	907, 864, 811	1188, 1100, 1075	877, 816, 812	1364, 1364, 1325
Criterion for observed reflections	$I > 2\sigma(I)$	$I > 2\sigma(I)$	$I > 2\sigma(I)$	$I > 2\sigma(I)$
R_{int}	0.0227	0.0382	0.0648	0.0000
θ_{max} (°)	67.48	65.03	67.61	67.61
Range of h, k, l	$-9 \rightarrow h \rightarrow 9$ $0 \rightarrow k \rightarrow 6$ $-13 \rightarrow l \rightarrow 0$	$0 \rightarrow h \rightarrow 8$ $-6 \rightarrow k \rightarrow 0$ $-17 \rightarrow l \rightarrow 16$	$0 \rightarrow h \rightarrow 9$ $0 \rightarrow k \rightarrow 5$ $-12 \rightarrow l \rightarrow 12$	$-8 \rightarrow h \rightarrow 0$ $0 \rightarrow k \rightarrow 38$ $0 \rightarrow l \rightarrow 6$
No. and frequency of standard reflections	3, every 100 reflections	3, every 100 reflections	3, every 100 reflections	3, every 100 reflections
Intensity decay (%)	2	0	2	2
Refinement				
Refinement on	F^2	F^2	F^2	F^2
$R[F^2>2\sigma(F^2)]$, $wR(F^2)$, S	0.0592, 0.1634, 1.439	0.0300, 0.0945, 0.913	0.0425, 0.1368, 1.387	0.0550, 0.1724, 1.640
No. of reflections and parameters used in refinement	864, 90	1100, 145	816, 100	1364, 137
H-atom treatment	Mixed	Mixed	Mixed	Mixed
Weighting scheme	$w = 1/[\omega^2(F_o^2) + (0.1P)^2]$, where $P = (F_o^2 + 2F_c^2)/3$	$w = 1/[\sigma^2(F_o^2) + (0.1000P)^2 + 0.0000P]$, where $P = (F_o^2 + 2F_c^2)/3$	$w = 1/[\omega^2(F_o^2) + (0.1P)^2]$, where $P = (F_o^2 + 2F_c^2)/3$	$w = 1/[\sigma^2(F_o^2) + (0.1P)^2]$, where $P = (F_o^2 + 2F_c^2)/3$
$(\Delta/\sigma)_{max}$	0.249	0.002	0.091	0.177
$\Delta\rho_{max}$, $\Delta\rho_{min}$(e Å^{-3})	0.568, −0.521	0.305, −0.190	0.655, −0.389	0.470, −0.351
Extinction method	None	*SHELXL*	*SHELXL*	*SHELXL*
Extinction coefficient	–	0.040 (4)	0.187 (19)	0.016 (3)

Computer programs used: *MSC/AFC* (Molecular Structure Corporation, 1991); *SHELXS*97 (Sheldrick, 1997*a*); *SHELXL*97 (Sheldrick, 1997*b*).

observed; in other words, the amide group does not affect the conformation of aliphatic, aromatic or polar side chains significantly. Their conformations would be flexible within the respective allowable angles and depend on the crystal packing and intermolecular interaction.

3.2. Crystal structures

The possible hydrogen bonds and some short contacts in the respective crystal structures are summarized in Table 4. The crystal packings could be grouped into three patterns, according to the interaction modes between the Cl ions and C-amide NH_2 groups (discussed later). As is exemplified in the crystal structure of $TrpNH_2$·HCl (Fig. 2*a*), the most frequently observed packing is in such a way that the amino and amide groups of neighbouring C-amides are located face-to-face in the same side. This interfacing region is stabilized to one another by the interaction with the Cl ions positioning among the neighbouring C-amides, forming a hydrophilic layer along a crystallographic axis. Consequently, the indole side chains form a hydrophobic stacking layer, thus leading to the formation of two different layers. Similar crystal packings have been formed in $ArgHN_2$·HCl, $GlnNH_2$·HCl, $MetNH_2$·HCl, $ValNH_2$·HCl and $IleNH_2$·HCl. Slightly different crystal packing is observed in $SerNH_2$·HCl (Fig. 2*b*). The antiparallel ladder-like molecular associations are formed by the hydrogen bonds of the side chain OH groups with amide NH_2 groups and Cl ions, forming two alternatively arranged layers of chloride ions and C-amide molecules.

On the other hand, $ThrNH_2$·HCl forms the another type of crystal packing (Fig. 2*c*). This is due to the different interaction mode between the Cl ions and amide NH_2 groups. As discussed later, the Cl ions in this crystal are bifurcately hydrogen-bonded to two neighbouring NH_2 groups translated

Table 2
Some selected bond lengths (Å) and angles (°).

C1′—N2, ∠C1—C1′—N2 and ∠N2—C1′—O1′ for C-amides and C1′—O2, ∠C1—C1′—O2 and ∠O2—C1′—O1′ for C-acids.

N1—C1	C1—C1′	C1′—O1′ C1′—O2	C1′—N2	∠N1—C1—C1′	∠C1—C1′—O1′	∠C1—C1′—N2	∠N2—C1′—O1′ ∠C1—C1′—O2	∠O2—C1′—O1′
$IleNH_2$·HCl	1.487 (5)	1.523 (7)	1.211 (7)	1.347 (8)	106.6 (4)	120.9 (5)	115.7 (5)	123.4 (6)
IleOH·HCl	1.504	1.535	1.210	1.284	108.6	120.0	113.3	126.8
$ValNH_2$	1.497 (3)	1.514 (4)	1.233 (3)	1.327 (4)	107.2 (2)	119.8 (2)	117.0 (2)	123.1 (1)
ValOH·HCl	1.494	1.509	1.201	1.309	106.2	123.7	112.4	123.9
	1.486	1.520	1.200	1.310	106.8	123.2	112.3	124.5
$ThrNH_2$	1.487 (5)	1.531 (5)	1.233 (5)	1.322 (5)	107.9 (2)	120.6 (2)	115.4 (2)	124.1 (2)
$SerNH_2$	1.495 (5)	1.500 (6)	1.247 (6)	1.324 (6)	108.0 (3)	120.3 (4)	117.2 (4)	122.4 (4)
$MetNH_2$	1.494 (6)	1.522 (8)	1.214 (8)	1.335 (8)	107.8 (5)	121.0 (6)	115.4 (6)	123.5 (6)
MetOH·HCl	1.508	1.512	1.197	1.321	106.9	124.4	110.5	125.1
$TrpNH_2$	1.483 (3)	1.507 (3)	1.220 (3)	1.334 (4)	108.0 (1)	121.4 (2)	115.9 (2)	122.6 (2)
TrpOH·HCl	1.505	1.540	1.147	1.325	107.0	125.7	106.8	127.5
$GlnNH_2$	1.499 (4)	1.525 (5)	1.220 (5)	1.330 (5)	107.2 (3)	120.4 (3)	115.1 (4)	124.5 (4)
GlnOH·HCl	1.510	1.535	1.208	1.296	108.0	123.7	112.2	124.1
$ArgNH_2$	1.480 (5)	1.532 (6)	1.222 (5)	1.317 (6)	107.4 (3)	121.4 (4)	115.8 (4)	122.8 (4)
Average								
C-amide	1.490 (6)	1.519 (9)	1.225 (10)	1.330 (8)	107.5 (4)	120.7 (5)	115.9 (7)	123.3 (6)
C-acid	1.501 (8)	1.525 (12)	1.194 (21)	1.308 (14)	107.3 (8)	123.5 (17)	111.3 (22)	125.3 (14)

Table 3
Selected torsion angles (°) of C-amidated amino acids, together with the C-unamidated ones (free forms and HCl salts) for comparison.

ψ: N1—C1—C1′—N2 for C-amides and N1—C1—C1′—O2 for C-acids. The conformation of the side chain follows the usual definition of amino acids [χ_1, N1—C1—C2—C3 (N1—C1—C2—O3 for Ser); χ_2, C1—C2—C3—C4 (C1—C2—C3—S4 for Met); χ_3, C2—C3—S4—C5 for Met, C2—C3—C4—N6 for Gln and Arg; χ_4, C3—C4—N5—C6; χ_5, C4—N5—C6—N8].

	ψ	χ_1	χ_2	χ_3	χ_4	χ_5
$IleNH_2$·HCl	129.5 (5)	−62.6 (5)	166.0 (7)			
IleOH·HCl	167.1	70.1	60.6			
Ile	164.0					
$ValNH_2$·HCl	157.0 (2)	63.5 (5)				
ValOH·HCl	−174.2	71.6				
Val	163.0	81.8				
$ThrNH_2$·HCl	161.8 (3)	−66.1 (3)				
Thr	156.1	−174.5				
$SerNH_2$·HCl	161.9 (5)	75.4 (4)				
Ser	−178.1	61.5				
$MetNH_2$·HCl	147.8 (6)	−170.2 (5)	179.7 (5)	−77.8 (4)		
MetOH·HCl	176.9	61.3	−178.2	68.7		
Met	163.7	−166.1	174.2	179.7		
	150.8	−165.6	73.6	73.6		
$TrpNH_2$·HCl	173.6 (2)	57.7 (2)	77.7 (3)			
TrpOH·HCl	173.9	−62.7	−78.0			
$GlnNH_2$·HCl	133.9 (3)	−69.1 (3)	−178.7 (4)	158.1		
GlnOH·HCl	162.8	−71.2	−170.3	−166.8		
Gln	168.6	70.5	176.1	164.8		
$ArgNH_2$·HCl	175.2 (4)	66.4 (3)	174.6 (4)	−178.4 (4)	−89.2 (4)	178.7 (5)
ArgO·HCl	174.2	−58.9	−164.4	179.3	−84.0	−170.3
	154.9	−52.8	173.2	−175.5	96.7	166.3

by a diad screw symmetry, while most of the other crystals form the bifurcated hydrogen bonds of Cl ions to two neighbouring amide NH_2 groups translated by one unit-cell. Consequently, the Cl ions are evenly distributed in the crystal lattice and the molecules are associated around these ions through the hydrogen bonds, thus forming a column along the *c* axis.

3.3. C*α*—H···O hydrogen bonds and carbonyl–carbonyl interactions

The C*α*—H···O [═C1—H···O1′] short contacts observed in the crystal structures of C-amides and C-acids are compared in Table 5. Judging from the summation (= 2.6 Å) of van der Waals radii of H and O atoms and the linearity of the C—H···O angle, these short contacts observed for C-amide·HCl crystals, except $ThrNH_2$, could be defined as hydrogen bonds; a typical interaction is shown in Fig. 3(*a*). Since such a C*α*—H···O hydrogen bond is also frequently observed in the crystal structures of the usual amino acids (Fig. 3*b*; see also Steiner, 1995) and other biomolecules (Wahl & Sundaralingam, 1997), this interaction may not necessarily result from the C-amidation. However, it is remarkable that the probability of forming such an interaction could be much higher for C-amides than C-acids (Table 5). The survey of the crystal structures of the usual oligopeptides indicates that the formation of such a C*α*—H···O interaction is restricted to the *β*-sheet structure (Fabiola *et al.*, 1997) or the C-terminal amino acid.

In the case of the zwitterionic state of the C-acids or the neutral state of the C-amides, the C1—H···O1′ interaction

usually accompanies the N1—H···O1′ (for the C-acid) or N2—H···O1′ (for the C-amide) interaction. However, such a coupled interaction is very rare in the crystal structures of HCl salts of both the C-amides and the -acids; in most cases a single interaction is formed. This clearly indicates that the hydrogen-bonding ability of Cα—H is strengthened by salt formation with HCl. Further, the hydrogen bonds to the amide NH_2 by two neighbouring chloride ions (discussed in the next section) appear to strengthen the Cα—H···O interaction significantly.

On the other hand, another feature to be noted is the intermolecular interaction between two neighbouring carbonyl C1′ and O1′ atoms, as shown in Fig. 4. Although this interaction is not necessarily formed in all crystal structures, most of them show the similar pattern of short contacts between the neighbouring amide C1′ and O1′ atoms. The C1′···O1′ distances in $IleNH_2$, $SerNH_2$, $TrpNH_2$, $GlnNH_2$ and $ArgNH_2$ (Table 4) are very close to the van der Waals separation distance (3.1 Å), and their intersecting angles of the C1′—O1′ bond with respect to the amide plane are 48, 29, 67, 84 and 43°, respectively. These contacts are all formed between the molecules translated by the twofold screw symmetry and the electrostatic interactions could be a driving force.

3.4. Characteristic binding mode of the Cl ion with C-amide

By salt formation with HCl, both C-amides and C-acids take the same electronic structure, *i.e.* the protonated amino group and the neutral amide/carboxyl group. However, the different number of H atoms between the amide NH_2 and carboxyl OH groups leads to the different binding modes with Cl ions. Fig. 5 shows four different interaction modes observed in the present crystal structures. The interaction mode of $IleNH_2$·HCl (Fig. 5*a*), the bifurcated hydrogen bonding of Cl ions to two neighbouring amide NH_2 groups translated by one unit-cell, is most frequently observed in the crystal structures

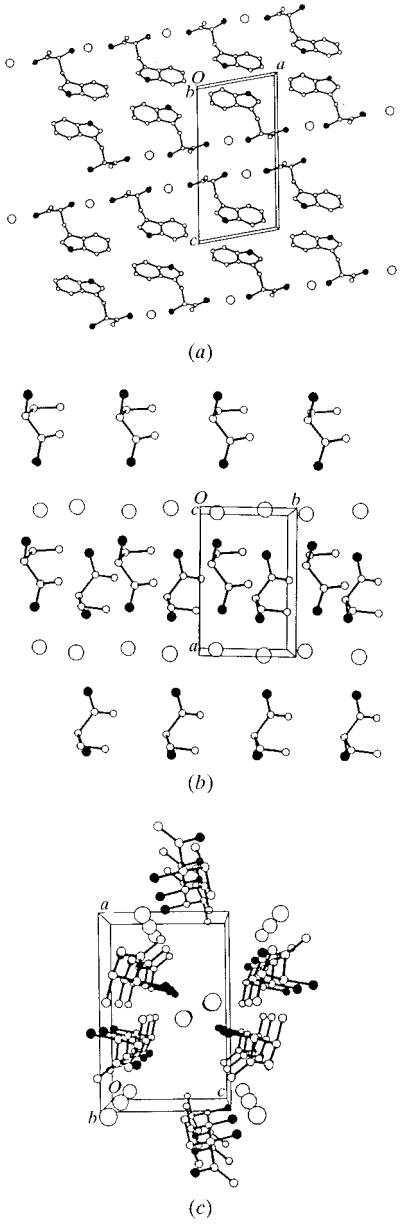

Figure 2
Perspective views of the crystal structures of (*a*) $TrpNH_2$·HCl, (*b*) $SerNH_2$·HCl and (*c*) $ThrNH_2$·HCl. The large open circles represent chloride ions and the N atoms are shown by the filled circles.

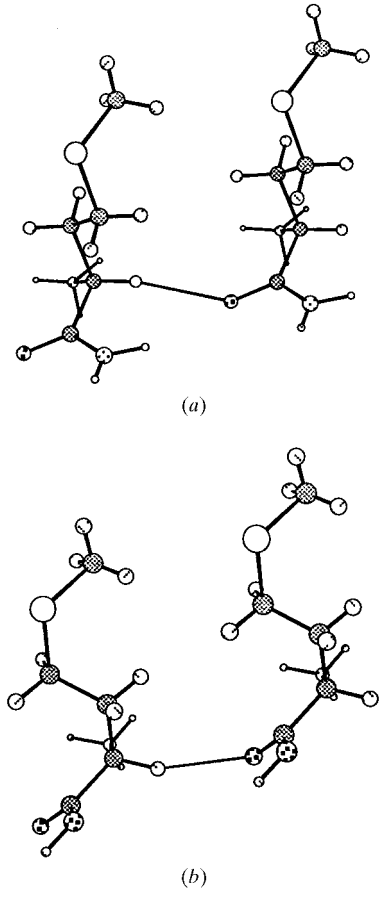

Figure 3
Stereoscopic views of the intermolecular Cα—H···O interactions in (*a*) $MetNH_2$·HCl and (*b*) MetOH·HCl. The shaded line shows hydrogen bonds. The open and meshed circles represent H and C atoms, respectively. The N and O atoms are shown by the circles marked with crosses and dots, respectively.

Table 4
Hydrogen bonds and some selected short contacts (except Cα—H···O).

Donor (D—H)	Acceptor (A)	Symmetry code	D···A (Å)	H···A (Å)	D—H···A (°)
IleNH$_2$·HCl					
N1	Cl1	$x-1, y, z$	3.173 (5)	2.27	164.1 (1)
N1	Cl1	$x-1, y+1, z$	3.123 (5)	2.18	174.8 (1)
N1	O1′	$-x, y+\frac{1}{2}, -z+1$	2.842 (6)	2.03	147.0 (3)
N2	Cl1	x, y, z	3.274 (5)	2.52	145.0 (1)
N2	Cl1	$x, y+1, z$	3.285 (5)	2.50	129.7 (1)
C1′	O1′	$-x, y+\frac{1}{2}, -z+1$	3.166 (7)		
ValNH$_2$·HCl					
N1	Cl1	$x-1, y-1, z$	3.166 (2)	2.29	168.87 (5)
N1	Cl1	$-x, y-\frac{1}{2}, -z+1$	3.209 (2)	2.42	154.46 (5)
N1	Cl1	$x, y-1, z$	3.580 (2)	2.55	165.78 (5)
N1	O1′	$-x, y-\frac{1}{2}, -z+1$	3.083 (3)	2.69	109.4 (1)
N2	Cl1	x, y, z	3.255 (3)	2.37	163.7 (7)
N2	Cl1	$x-1, y, z$	3.407 (3)	2.42	163.15 (7)
ThrNH$_2$·HCl					
N1	Cl	$1-x+\frac{3}{2}, -y+1, z+\frac{1}{2}$	3.155 (3)	2.21	169.37 (9)
N1	O4	$-x+\frac{3}{2}, -y+2, z+\frac{1}{2}$	2.965 (4)	2.15	146.5 (2)
N1	O1′	$x-\frac{1}{2}, -y+\frac{3}{2}, -z+1$	2.898 (4)	2.96	76.8 (2)
N2	Cl1	x, y, z	3.279 (4)	2.28	164.2 (1)
N2	Cl	$1-x+\frac{3}{2}, -y+1, z-\frac{1}{2}$	3.327 (4)	2.36	165.5 (1)
O4	Cl	$1-x+2, y+\frac{1}{2}, -z+\frac{1}{2}$	3.058 (3)	2.26	151.13 (8)
SerNH$_2$·HCl					
N1	Cl1	$x+1, y, z-1$	3.346 (4)	2.88	115.24 (9)
N1	Cl1	$-x+1, y-\frac{1}{2}, -z+1$	3.171 (4)	2.19	170 (1)
N1	Cl1	$-x+1, y+\frac{1}{2}, -z+1$	3.224 (4)	2.24	165.5 (1)
N1	O1′	$-x+1, y-\frac{1}{2}, -z$	2.786 (5)	2.08	138.9 (2)
N2	Cl1	$-x, y+\frac{1}{2}, -z+1$	3.255 (5)	2.24	171.6 (1)
N2	O3	$-x+1, y-\frac{1}{2}, -z+1$	2.948 (6)	2.07	139.5 (2)
C1′	O1′	$-x+1, y-\frac{1}{2}, -z$	3.102 (6)		
O1′	O1′	$-x+1, y-\frac{1}{2}, -z$	3.203 (5)		
O3	Cl1	$-x+1, y+\frac{1}{2}, -z+1$	3.126 (4)		
MetNH$_2$·HCl					
N1	Cl1	$-x+1, y+\frac{1}{2}, -z+2$	3.234 (5)	2.42	157.1 (1)
N1	Cl1	$-x+1, y-\frac{1}{2}, -z+2$	3.169 (5)	2.33	164.7 (3)
N1	Cl1	$x, y, z+1$	3.340 (5)	2.84	117.0 (1)
N2	Cl1	$-x+2, y-\frac{1}{2}, -z+2$	3.403 (6)	2.62	137.3 (1)
N2	Cl1	$-x+2, y+\frac{1}{2}, -z+2$	3.347 (6)	2.70	158.3 (1)
O1′	C1	$x, y+1, z$	3.251 (7)		
TrpNH$_2$·HCl					
N1	Cl1	$x+1, y, z$	3.347 (2)	2.47	149.25 (5)
N1	Cl1	$x+1, y-1, z$	3.173 (2)	2.25	160.28 (6)
N1	Cl1	$-x, y-\frac{1}{2}, -z+1$	3.152 (2)	2.30	157.94 (6)
N2	Cl1	$x, y-1, z$	3.528 (3)	2.62	159.65 (6)
N2	Cl1	x, y, z	3.269 (3)	2.33	176.68 (6)
N2	O1′	$-x, y-\frac{1}{2}, -z+1$	3.390 (3)		
C1′	O1′	$-x, y-\frac{1}{2}, -z+1$	3.371 (3)		
GlnNH$_2$·HCl					
N1	Cl1	$-x+1, y+\frac{1}{2}, -z+1$	3.153 (3)	2.31	167.33 (8)
N1	Cl1	$-x+1, y-\frac{1}{2}, -z+1$	3.186 (3)	2.33	171.42 (8)
N1	O1′	$-x+1, y+\frac{1}{2}, -z+2$	2.819 (4)	1.97	161.8 (2)
N1	Cl1	$x+1, y, z+1$	3.440 (3)		
N2	Cl1	$-x, y-\frac{1}{2}, -z+1$	3.361 (4)	2.53	146.45 (9)
N2	Cl1	$-x, y+\frac{1}{2}, -z+1$	3.338 (4)	2.86	113.7 (8)
N2	N6	$-x+1, y-\frac{1}{2}, -z+1$	3.352 (5)		
N6	Cl1	$x+1, y, z$	3.370 (4)	2.48	153.08 (9)
N6	O5	$x, y+1, z$	2.972 (5)	2.35	118.1 (2)
C1′	O1′	$-x+1, y+\frac{1}{2}, -z+2$	3.118 (4)		
O1′	O1′	$-x+1, y-\frac{1}{2}, -z+2$	3.387 (4)		
ArgNH$_2$·HCl					
N1	Cl1	$x-1, y, z$	3.296 (3)	2.32	173.6 (1)
N1	Cl1	$x-1, y, z+1$	3.197 (3)	2.33	173.6 (1)
N1	O1′	$-x+\frac{1}{2}, -y+2, z+\frac{1}{2}$	2.925 (4)	2.15	143.0 (2)
N1	Cl1	$-x+\frac{1}{2}, -y+2, z+\frac{1}{2}$	3.372 (3)	3.01	106.03 (9)

Table 4 (continued)

Donor (D—H)	Acceptor (A)	Symmetry code	D···A (Å)	H···A (Å)	D—H···A (°)
N2	Cl1	x, y, z	3.227 (5)	2.29	153.3 (1)
N2	O1W	$x, y, z+1$	2.965 (6)	2.26	156.8 (3)
O1W	Cl1	x, y, z	3.168 (4)		
O1W	Cl2	x, y, z	3.255 (4)		
N5	Cl2	x, y, z	3.224 (4)	2.31	149.5 (1)
N7	Cl2	$x-1, y, z$	3.220 (4)	2.38	165.3 (1)
N7	O1W	$x-1, y, z+1$	2.938 (5)	2.21	162.8 (3)
N8	Cl2	$x-1, y, z$	3.234 (4)	2.22	156.8 (1)
N8	Cl2	$x-\frac{1}{2}, -y+\frac{3}{2}, -z+1$	3.225 (4)	2.61	122.8 (1)
C1′	O1′	$-x+\frac{1}{2}, -y+2, z+\frac{1}{2}$	3.221 (5)		
O1′	O1′	$-x+\frac{1}{2}, -y+2, z+\frac{1}{2}$	3.377 (4)		

of C-amides, *i.e.* ValNH$_2$·HCl, MetNH$_2$·HCl, TrpNH$_2$·HCl, GlnNH$_2$·HCl and LysNH$_2$·2HCl (Cruz *et al.*, 1991). In ThrNH$_2$·HCl (Fig. 5*b*) the Cl ions are bifurcately hydrogen-bonded to two neighbouring NH$_2$ groups translated by a diad screw symmetry. In the crystal structure of ArgNH$_2$·HCl (Fig. 5*c*) or SerNH$_2$·HCl (Fig. 5*d*), a water solvent or the OH group of the Ser side chain participates in the interaction mode similar to that in Fig. 5(*b*), respectively. It is important to note that all these interaction modes lead the C-amide molecules into a 'head-to-head' parallel arrangement and this could be a unique binding mode of Cl ions by the C-terminal amide group. Although similar bifurcated hydrogen bonds could also be formed between the Cl ions and the protonated amino NH_3^+ group, this $NH_3^+\cdots Cl\cdots NH_3^+$ interaction mode could not reflect well the structural feature of the C-amides, because the same mode is commonly observed in the crystal structures of C-acid HCl salts.

On the other hand, the structural features of C-acid HCl salts could be characterized by the interaction between the

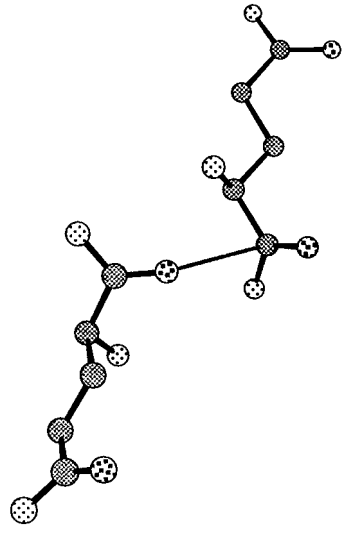

Figure 4
Stereoscopic view of the intermolecular C1′···O1′ short contact between the carbonyl groups translated by diad-screw symmetry, observed in the crystal structure of GlnNH$_2$·HCl. The shaded line shows interatomic short contacts. The N and O atoms are shown by the circles marked with crosses and dots, respectively.

carboxyl OH group and the Cl ion. Two typical interaction patterns are shown in Figs. 6(*a*) and (*b*). The neutral carboxyl OH is hydrogen-bonded to a chloride anion and this ion further interacts with neighbouring donor groups of NH_3^+ and/or water OH through hydrogen bonds or electrostatic interactions. The same interaction mode is also observed in the crystals of ValOH·HCl, MetOH·HCl and TrpOH·HCl. This type of interaction *via* the Cl ion leads to a 'head-to-tail' arrangement of C-acid molecules, which is different from the head-to-head molecular arrangement of C-amides. In the case of the carboxylic group being in an anionic state, like ArgOH·HCl, such an interaction is not formed and thus may depend on the electronic state of the amino acid side chain.

Based on the above-mentioned interaction modes with Cl ions, it would be reasonable to assume that the amide group can trap the biological anion in such a way that two amide groups sandwich the anion. Such a tight fixation of the anion is impossible in the case of the carboxyl group, because most of the amino acids or peptides have a zwitterionic structure in the living cell.

4. General discussion

The present crystal structures showed that the C-amidation of amino acid leads to a different interaction with Cl ions from that in the amino acid and this is probably due to the different physicochemical behaviour, especially the different hydrogen-bonding ability, between the amide and carboxyl groups. To make clear the structural difference of both groups for hydrogen-bond formation, the spatial distribution of the polar atoms/groups which are hydrogen-bonded to the amide or carboxyl group is shown in Fig. 7(*a*) and (*b*), respectively. This figure indicates a clear difference concerning the hydrogen-bonding patterns of the amide and carboxyl groups. Although there is insufficient data, Fig. 7(*a*) indicates that the amide NH_2 group simultaneously forms two hydrogen bonds with the acceptor atoms of neighbouring molecules or Cl ions and their spatial dispositions are almost separated into two regions. Characteristically, one of the two NH bonds, which is parallel to the C1—C1′ bond, severely restricts the position of the acceptor atom to form a linear hydrogen bond, as compared

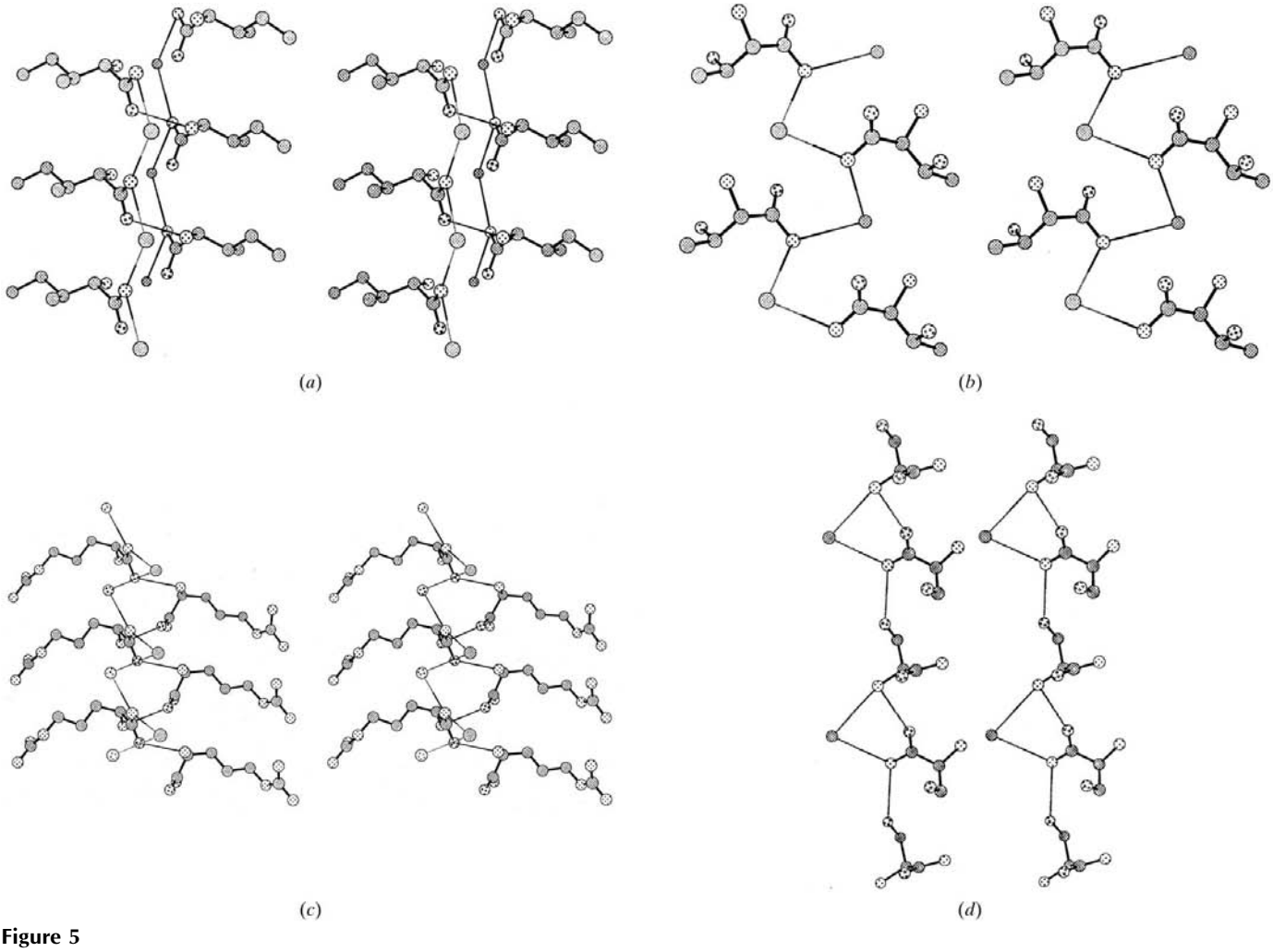

Figure 5
Stereoscopic views of the interaction patterns between the amide NH_2 groups and chloride ions, observed in the crystal structures of (*a*) $IleNH_2$·HCl, (*b*) $ThrNH_2$·HCl, (*c*) $ArgNH_2$·HCl and (*d*) $SerNH_2$·HCl. The shaded lines show hydrogen bonds. The N and O atoms are shown by the circles marked with crosses and dots, respectively. The chloride ions and water solvents are shown by the shaded and cross-marked balls, respectively.

with the other bond, the acceptor atom of which is relatively widely distributed, suggesting non-equivalent hydrogen-bonding ability in the NH_2 group. In contrast, the amide O1′ forms one to two hydrogen bonds with the donor groups that are widely distributed so as to surround the O atom. It appears noteworthy that these acceptor atoms are not located on the amide plane, but tetrahedrally displaced with respect to the plane.

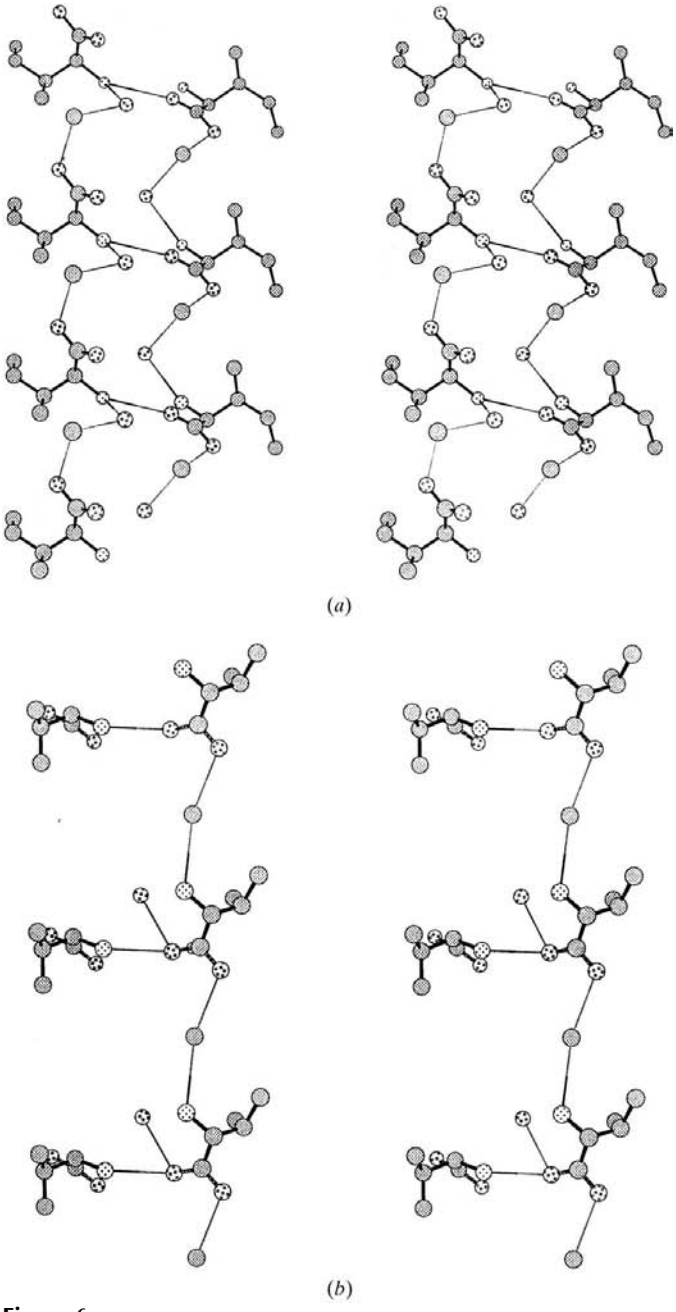

Figure 6
Stereoscopic views of interaction patterns between the carboxyl OH groups and chloride ions, observed in the crystal structures of (*a*) IleOH·HCl and (*b*) ValOH·HCl. The shaded lines show hydrogen bonds. The N and O atoms are shown by the circles marked with crosses and dots, respectively. The chloride ions and water solvents are shown by the shaded and cross-marked balls, respectively.

Table 5
Comparison of Cα—H···O short contacts (Å) of C-amides and C-acids.

	C···O (Å)	H···O (Å)	C—H···O (°)
$IleNH_2$·HCl	3.330 (7)	2.49	143.4 (3)
IleOH·HCl	3.323	3.14	89.5
Ile	3.122	2.87	96.2
	3.456	2.93	115.1
$ValNH_2$·HCl	3.250 (3)	2.32	159.2 (1)
ValOH·HCl	3.356	2.52	137.4
Val	3.096	2.78	101.6
	3.317	2.44	154.1
$ThrNH_2$·HCl	3.349 (4)	2.86	111.9 (2)
Thr	3.276	2.35	160.0
$SerNH_2$·HCl	3.401 (5)	2.46	160.8 (2)
	3.143 (5)	2.99	89.7 (2)
Ser	3.368	2.79	118.3
	3.346	3.08	97.1
$MetNH_2$·HCl	3.251 (7)	2.29	167.5 (3)
MetOH·HCl	3.282	2.28	159.0
Met	3.313	2.63	126.8
	3.157	3.00	90.0
$TrpNH_2$·HCl	3.134 (3)	2.32	139.9 (1)
TrpOH·HCl	3.250	2.45	133.3
$GlnNH_2$·HCl	3.314 (4)	2.45	146.5 (2)
GlnOH·HCl†	3.146		
Gln	3.335	2.70	143.2
$ArgNH_2$·HCl	3.354 (5)	2.41	161.9 (2)
	3.050 (5)	2.61	107.8 (2)
$ArgO^-$·HCl‡	3.483	2.68	143.6

† The positions of the H atoms have not been deposited. ‡ The carboxyl group takes an anionic state.

In the case of the neutral carboxyl group (Fig. 7*b*), the spatial distribution of the donor group (NH or OH) which is hydrogen-bonded to the carboxyl O1′ could be roughly separated into two regions. Although this situation is similar to the case of the C-amide O1′, the hydrogen bonds appear to be rather weak because of the relatively wide distribution. On the other hand, the carboxyl OH group restricts the position of the acceptor atom (O or Cl^-) to a limited region so as to form linear O—H···O hydrogen bonds. There is no observation of the hydrogen bond, which is *cis* formed with respect to the C1—C1′ bond.

Based on the spatial distribution of such polar atoms or groups, the following discussion could be possible. In the binding of C-amides with partner molecules or ions, two hydrogen bonds *via* the amide NH_2 are first formed and then the amide O serves to further stabilize the interaction through the relatively weak and flexible hydrogen bond. On the other hand, in the case of the neutral carboxyl group, the interaction appears to be not so specific, because the binding is mainly performed through the single hydrogen bond of the carboxyl OH group. The present results would be useful upon considering why the C-amidation of peptides is necessary to reveal their activity. The hydrogen-bonding ability (including anion-binding ability) and its structural features of the C-amide group may be necessary to just fit to the receptor.

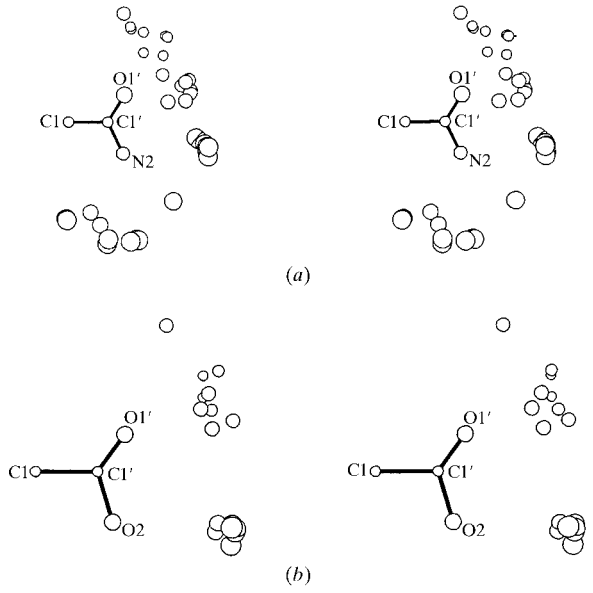

Figure 7
Stereoscopic views of the spatial distribution of polar atoms/groups which are hydrogen-bonded to (*a*) C-amide O1′ and N2H, or (*b*) C-acid O1′ and O2H. The hydrogen-bonding donor groups (OH, CH or NH_2) and acceptor (O and Cl^-) atoms are shown by open circles, the scales of which correspond to the atomic numbers.

References

Ando, O., Ashida, T., Sasada, Y. & Kakudo, M. (1967). *Acta Cryst.* **23**, 172–173.

Blasio, B. di, Pavone, V. & Pedone, C. (1977). *Cryst. Struct. Commun.* **6**, 845–848.

Cody, V. (1985) *Chemistry and Biochemistry of the Amino Acids*, edited by G. C. Barrett, pp. 625–653. New York: Chapman and Hall.

Cruz, X. De La, Tormo, J., Fita, I. & Subirana, J. A. (1991). *Acta Cryst.* C**47**, 1705–1707.

Dalhus, B. & Gorbitz, C. H. (1996). *Acta Chem. Scand.* **50**, 544–548.

Dow, J., Jensen, L. H., Mazumdar, S. K., Srinivasan, R. & Ramachandran, G. N. (1970). *Acta Cryst.* B**26**, 1662–1671.

Eipper, B. A. & Mains, R. E. (1988). *Annu. Rev. Physiol.* **50**, 333–344.

Fabiola, G. F., Nagarajan, K. V. & Pattabhi, V. (1997). *Acta Cryst.* D**53**, 316–320.

Görbitz, C. H. & Dalhus, B. (1996). *Acta Cryst.* C**52**, 1464–1466.

In, Y., Tani, S. & Ishida, T. (2000). *Chem. Pharm. Bull.* **48**, 374–381.

Kistenmacher, T. J., Rand, G. A. & Marsh, R. E. (1974). *Acta Cryst.* B**30**, 2573–2578.

Koetzle, T. F., Frey, M. N., Lehmann, M. S. & Hamilton, W. C. (1973). *Acta Cryst.* B**29**, 2571–2575.

Koetzle, T. F., Golic, L., Lehmann, M. S., Verbist, J. J. & Hamilton, W. C. (1974). *J. Chem. Phys.* **60**, 4690–4696.

Kulathila, R., Merkler, K. A. & Merkler, D. J. (1999). *Nat. Prod. Rep.* **16**, 145–154.

Merkler, D. J. (1994). *Enzyme Microb. Technol.* **16**, 450–456.

Molecular Structure Corporation (1991). *MSC/AFC*. MSC, 3200 Research Forest Drive, The Woodlands, TX 77381, USA.

North, A. C. T., Phillips, D. C. & Mathews, F. S. (1968). *Acta Cryst.* A**24**, 351–359.

Ramanadham, M., Sikka, S. K. & Chidambaram, R. (1973). *Pramana*, **1**, 247–259.

Shamala, N. & Venkatesan, K. (1972). *Cryst. Struct. Commun.* **1**, 227–229.

Sheldrick, G. M. (1997*a*). *SHELXS*97. University of Göttingen, Germany.

Sheldrick, G. M. (1997*b*). *SHELXL*97. University of Göttingen, Germany.

Steiner, T. (1995). *J. Chem. Soc. Perkin Trans 2*, pp. 1315–1319.

Suwan, S., Isobe, M., Yamashita, O., Minakata, H. & Imai, K. (1994). *Insect Biochem. Mol. Biol.* **24**, 1001–1007.

Takigawa, T., Ashida, T., Sasada, Y. & Kakudo, M. (1966). *Bull. Chem. Soc. Jpn*, **39**, 2369–2378.

Torii, K. & Iitaka, Y. (1973). *Acta Cryst.* B**29**, 2799–2807.

Varughese, K. I. & Srinivasan, R. (1976). *Pramana*, **6**, 189–195.

Wahl, M. C. & Sundaralingam, M. (1997). *Trends Biochem. Sci.* **22**, 97–102.